Trial-Level Regressor Modulation for Functional Magnetic Resonance Imaging Designs Requiring Strict Periodicity of Stimulus Presentations: Illustrated Using a Go/No-Go Task

Magnetic Resonance Insights
Volume 10: 1–7

DOI: 10.1177/1178623X17746693

Michael A Motes[1], Neena K Rao[1], Ehsan Shokri-Kojori[1], Hsueh-Sheng Chiang[1], Michael A Kraut[2] and John Hart Jr[1,3]

[1]School of Behavioral and Brain Sciences, University of Texas at Dallas, Dallas, TX, USA. [2]Department of Radiology, Johns Hopkins University, Baltimore, MD, USA. [3]Department of Neurology, University of Texas Southwestern Medical Center, Dallas, TX, USA.

ABSTRACT: Computer-based assessment of many cognitive processes (eg, anticipatory and response readiness processes) requires the use of invariant stimulus display times (SDT) and intertrial intervals (ITI). Although designs with invariant SDTs and ITIs have been used in functional magnetic resonance imaging (fMRI) research, such designs are problematic for fMRI studies because of collinearity issues. This study examined regressor modulation with trial-level reaction times (RT) as a method for improving signal detection in a *go/no-go* task with invariant SDTs and ITIs. The effects of modulating the *go* regressor were evaluated with respect to the detection of BOLD signal-change for the *no-go* condition. BOLD signal-change to *no-go* stimuli was examined when the *go* regressor was based on a (a) canonical hemodynamic response function (HRF), (b) RT-based amplitude-modulated (AM) HRF, and (c) RT-based amplitude and duration modulated (A&DM) HRF. Reaction time–based modulation reduced the collinearity between the *go* and *no-go* regressors, with A&DM producing the greatest reductions in correlations between the regressors, and greater reductions in the correlations between regressors were associated with longer mean RTs and greater RT variability. Reaction time–based modulation increased statistical power for detecting group-level *no-go* BOLD signal-change across a broad set of brain regions. The findings show the efficacy of using regressor modulation to increase power in detecting BOLD signal-change in fMRI studies in which circumstances dictate the use of temporally invariant stimulus presentations.

KEYWORDS: FMRI, regression modeling, response inhibition

RECEIVED: July 25, 2017. **ACCEPTED:** November 13, 2017.

TYPE: Methodology

FUNDING: The author(s) received no financial support for the research, authorship, and/or publication of this article.

DECLARATION OF CONFLICTING INTERESTS: The author(s) declared no potential conflicts of interest with respect to the research, authorship, and/or publication of this article.

CORRESPONDING AUTHOR: Michael A Motes, School of Behavioral and Brain Sciences, University of Texas at Dallas, 1966 Inwood Road, Dallas, TX 75235, USA. Email: michael.motes@utdallas.edu

For many psychological assessments, the engagement of a cognitive process of interest requires the temporal regularity of stimulus presentations in the form of invariant stimulus display times (SDT) and intertrial intervals (ITI). Temporal variability in stimulus presentations has been shown to affect the engagement of a host of processes, including task switching,[1] response preparation,[2,3] and response inhibition.[4–6] The requirement of temporally invariant stimulus presentations, however, seemingly renders such paradigms impracticable for fMRI studies due to extreme collinearity, and possibly singularity, between the condition regressors used in conventional techniques for deconvolving fMRI time series data[7,8] (where collinearity can lead to error in estimating fMRI signal-change with the general linear modeling approach). For this study, fMRI data collected on participants who completed a *go/no-go* task were used to illustrate the use of trial-level regressor modulation as a method for reducing regressor collinearity and improving signal detection in designs requiring temporally regular stimulus presentations.

Temporal variability in stimulus presentations has been shown to affect response execution and inhibition in *go/no-go* paradigms.[4,6] *Go/no-go* tasks typically involve building preparatory or anticipatory cognitive and motor responses through the frequent and temporally regular presentations of *go* stimuli to which participants are to respond and then involve the attenuation, circumvention, or "control" of the prepotent responses to less frequently presented *no-go* stimuli. Varying the ITI in *go/no-go* tasks at 10%, 30%, and 50% of the mean ITI ($M = 1000$ ms; *go* trials = 75%) has been shown to lead to increases in reaction time (RT) and increases in RT variability, at least for men, and varying the ITI has been shown to lead to reductions in commission error rates at 10% with systematic increases in commission error rates (ie, responding to *no-go* stimuli) at 30% and 50%.[6]

Although designs with invariant SDTs and ITIs might be necessary for engagement of some processes, such designs are problematic for fMRI, in part, due to regressor collinearity affecting the estimation of BOLD signal-change obtained at the subject level in conventional fMRI data analysis. In conventional fMRI data analysis, ordinary least squares multiple regression is used to obtain BOLD signal-change estimates for each experimental condition by regressing the BOLD time series on condition regressors on a voxel-wise basis. Condition regressors are created by convolving an idealized hemodynamic response function (HRF) with condition stimulus event

functions (ie, impulse response functions occurring at each trial onset). That is,

$$y(t) = \sum_{k=1}^{K} h(t - \tau_k) \quad (1)$$

where t is the time in the time series, k is the trial for the condition, τ_k is the time of the onset of the kth trial for the condition, and $h(t-\tau_k)$ is the convolution of an idealized HRF with the condition stimulus event function, eg, $h(t-\tau_k) = (t-\tau_k)^{8.6} \cdot e^{-(t-\tau_k)/0.547}$.[7]

Through multiple regression, BOLD signal-change estimates then are partial slopes relating the orthogonalized condition regressors to the BOLD time series. That is, in matrix form with standardized variables (ie, mean-centered with unit variance),

$$\hat{\beta} = (X'X)^{-1}(X'y) = R_{xx}^{-1}R_{xy} \quad (2)$$

where signal-change estimates (ie, $\hat{\beta}$) are a function of the product of the inverse of the matrix of correlations between predictors (ie, R_{xx}^{-1}) and the matrix of correlations between predictors and the time series (ie, R_{xy}) or expressed in a simplified, 2-variable form:

$$\hat{\beta}_{y1\cdot 2} = \frac{r_{y1} - r_{y2}r_{12}}{1 - R_{12}^2} \quad (3)$$

where r_{y1} and r_{y2} are the correlation coefficients for y correlated with 2 different condition regressors, r_{12} is the correlation coefficient between the 2 condition regressors, and R_{12}^2 is the proportion of shared variance between the 2 condition regressors.

From the partial slope formulas, it is clear that the signal-change estimates are affected by the direction and magnitude of collinearity between the regressors and the direction and magnitude of correlations between the time series and the other predictors if collinearity is present. The magnitude of errors in estimating partial slopes has been shown to be affected by the direction and magnitude of the collinearity, sample size, and fit of the full model.[9,10] The effects of high collinearity ($r = .95$) have been shown to be substantially higher with smaller sample sizes (eg, number of time points ≤100) and the fit of a moderate full model (eg, $R^2 \leq 0.50$), at least, based on simulation parameters examined.[9] For fMRI analyses, increased error in estimating the partial slopes then can affect statistical power in group-level analyses, where partial slopes per participant per condition are used as task-related or process-related BOLD signal-change estimates.

This issue of collinearity has been acknowledged in the fMRI *go/no-go* literature.[11,12] In fMRI studies, blocked designs with varying proportions of *no-go* trials between blocks, slow event-related designs, and rapid event-related designs with and without varied ITIs have been used. However, the designs used have limitations regarding the inferences that can be drawn about inhibition processes. With blocked designs, for instance, state-level versus trial-level inhibition processes cannot be disentangled (ie, states of preparedness to respond develop over sets of trials),[13] and process engagement frequencies cannot be easily balanced across blocks (eg, motor response frequencies differ with no-go proportions). With slow event-related designs and rapid event-related designs with varied ITIs, slowing or varying the stimulus presentation rate could affect the establishment of the prepotent *go* response, as shown in the studies examining RT and commission errors.[6]

One analytical approach has been to exclude modeling the *go* trials in the analysis and treat *go*-related periods as part of the implicit baseline.[14–16] This approach, however, has limitations regarding the inferences that can be drawn about inhibition processes. *No-go* signal-change estimates, for instance, could be affected by the influence of the mean of the *go*-related signal-change on the implicit baseline and the influence of the mean of the *go*-related signal-change on the total variance in the data. In addition, the interpretation of the direction of the effects from such an analysis would be ambiguous. Positive correlations between BOLD and the *no-go* regressor could occur due to increased regional BOLD signal-change from baseline in response to the *no-go* stimulus or to the signal returning to baseline from a period of decreased signal-change (ie, "deactivation") in response to the *go* stimuli. Furthermore, when collinearity is present, omitting one of the correlated predictors biases the parameter estimate for the predictor left in the regression model, even with large samples (eg, n = 500), and the magnitude of the bias monotonically increases with the magnitude of the collinearity.[10]

Although varying ITIs would affect the processes engaged in a *go/no-go* task,[4–6] the duration of engaged processes does vary from trial-to-trail, and RT variability has been used as an index of variability in processing time.[4,6] Introducing model variability into the *go* regressor by varying trial-level HRFs by RT could be used to reduce collinearity between the *go* and *no-go* regressors and thus improve the unique variance accounted for by each regressor. In addition, hemodynamic response regressors modulated by trial RTs have the potential for better accounting for BOLD signal-change than typically used non-modulated models because RT-scaled models might better reflect the underlying duration of the neural activity.[17] Thus, in voxels in which neurons are responding to both *go* and *no-go* trials, a potentially better fitting *go* model will provide more stable *no-go* partial slope estimates across participants and thus increase group-level statistical power. Increased stability would come from the reduction in the variance in y to be explained by the *no-go* regressor after removing shared variance with the *go* regressor.

This study examined the use of RT modulation when analyzing fMRI time series data collected using a rapid event-related *go/no-go* task with constant SDTs and ITIs. Two RT modulation methods were explored. For one method, the amplitude of the canonical HRF for a trial was scaled proportionally to the RT for the trial, and for the other, the amplitude

and width of the idealized HRF for a trial were scaled proportionally for the RT for the trial. Thus, the effects of RT modulation of the *go* regressor on the independence of the *no-go* regressor and on the detection of group-level *no-go* effects were examined. Decorrelating the *no-go* model from the *go* model, by creating *go* model trial-by-trial uniqueness with RT modulation, would allow for increased uniqueness in the sampling of BOLD responses to account for the unknown signal-change parameter estimates on the *no-go* trials.

Methods

Participants

A total of 16 healthy young adults participated (women = 10; mean age = 23.5 years; range = 19-34 years). All participants were prescreened for magnetic resonance imaging contraindications and for medical, neurologic, and psychiatric illness, and all had either normal or corrected-to-normal visual acuity. All participants gave written informed consent in accordance with a protocol approved by the Institutional Review Boards of the University of Texas Southwestern Medical Center and the University of Texas at Dallas. The research was conducted in accordance with the principles expressed in the Declaration of Helsinki. Analyses of the full set of data examining inhibition under varying categorization requirements have been reported in another publication.[18]

Stimuli

Participants completed several tasks while in the scanner, but for this study, only the data from one run of the *go/no-go* task were analyzed. A car served as the *go* stimulus, and a dog served as the *no-go* stimulus. Both were black line drawings on white backgrounds, and they were taken from a standardized picture set.[19] Stimuli were projected onto a screen at the rear of the bore of the scanner and viewed by participants via an angled mirror (approximately 45°) positioned above the receiving coil, with the midpoint of the mirror approximately 12 cm from the participant's eyes. E-Prime (Psychology Software Tools, Pittsburgh, PA, USA) was used to control stimulus presentations and to record responses and RTs, and responses were given via a magnetic resonance–compatible response box.

Procedure

Participants were instructed to respond as quickly and accurately as possible to *go* stimuli and to withhold responding to *no-go* stimuli. There were 160 (80%) *go* trials and 40 *no-go* trials. The SDT was 250 ms followed by a centered, fixation cross over a 1750-ms ITI.

fMRI data acquisition parameters

Brain imaging data were acquired on a Philips 3T Achieva scanner with an 8-element, SENSE, receive-only head coil. The fMRI data were acquired in the transverse plane, using an EPI sequence: repetition time (TR) = 1.5 seconds, echo time (TE) = 25 ms, flip angle = 60°, 36 slices/volume, 289 volumes/run, slice thickness = 4 mm with no gap, interleaved acquisition inferior to superior, and acquisition matrix = 64 voxels × 64 voxels at 3.44 mm × 3.44 mm. High-resolution anatomical images also were acquired for image registration (MPRAGE; 1-mm isovoxel; sagittal; TE = 3.7 ms; flip angle = 12°).

Illustration and Evaluation of Regressor Collinearity

Figure 1A.1 illustrates the regressor collinearity problem for the *go/no-go* task. Idealized BOLD signal-change models for a typical *go/no-go* task with fixed SDTs and ITIs are depicted: *go* trials = 80%, *no-go* trials = 20%, stimulus duration = 250 ms, ITI = 1750 ms, and TR = 1.5 seconds for the fMRI acquisition sequence (ie, the parameters used in the present study). Each idealized *go* and *no-go* regressor (Figure 1A.1) was created by convolving a canonical HRF with *go* and *no-go* stimulus event functions (ie, impulse functions occurring at each trial onset), see equation (1).

The resulting *go* and *no-go* regressors were significantly negatively correlated, $r(n = 289) = -.48$ (Figure 1A.2), but this obtained correlation coefficient actually underestimated the strength of the linear relationship between the 2 models due to data points at the beginning (circled by a gray solid line) and end (circled by a gray dashed line) of each model having undue influence on the assessment of the linear relationship. In the beginning of the run, the *go* model increased with no corresponding changes in the *no-go* model. Afterward, *go* and *no-go* models become perfectly negatively correlated until the end of the run, $r(n = 260) = -.99$, only reduced from 1.00 due to temporal resampling. At the end of the run, the models then become positively correlated as the hemodynamic responses are expected to return to baseline.

Three subsequent regression models were evaluated. For the first model, *deleted trials* (DT), trials in which omission errors occurred on *go* trials, commission errors occurred on *no-go* trials, and *go* trials in which RTs were ±2.5 SDs from the mean RT for the participant were excluded from the stimulus event functions in building the *go* and *no-go* regressors. For the correct *go* trials, 2 additional regressor models were then constructed. For the *amplitude modulated* (AM) model, the heights of the δ-functions were scaled proportional to the participant's mean RT before the event function was convolved with the canonical HRF. That is,

$$y(t) = \sum_{k=1}^{K} (a_k - \bar{a}) h(t - \tau_k) \qquad (4)$$

where t is the time in the time series, k is the trial for the condition, a_k is the RT for the kth trial, $\bar{a}$ is the mean RT, τ_k is the time of the onset of the kth trial for the condition, and $h(t-\tau_k) = (t-\tau_k)^{8.6} \cdot e^{-(t-\tau_k)/0.547}$.[8] For the *amplitude and duration modulated* (A&DM), boxcar functions were created for each trial, with the duration of the boxcar lasting from the trial onset to the time of the response, and the boxcar functions

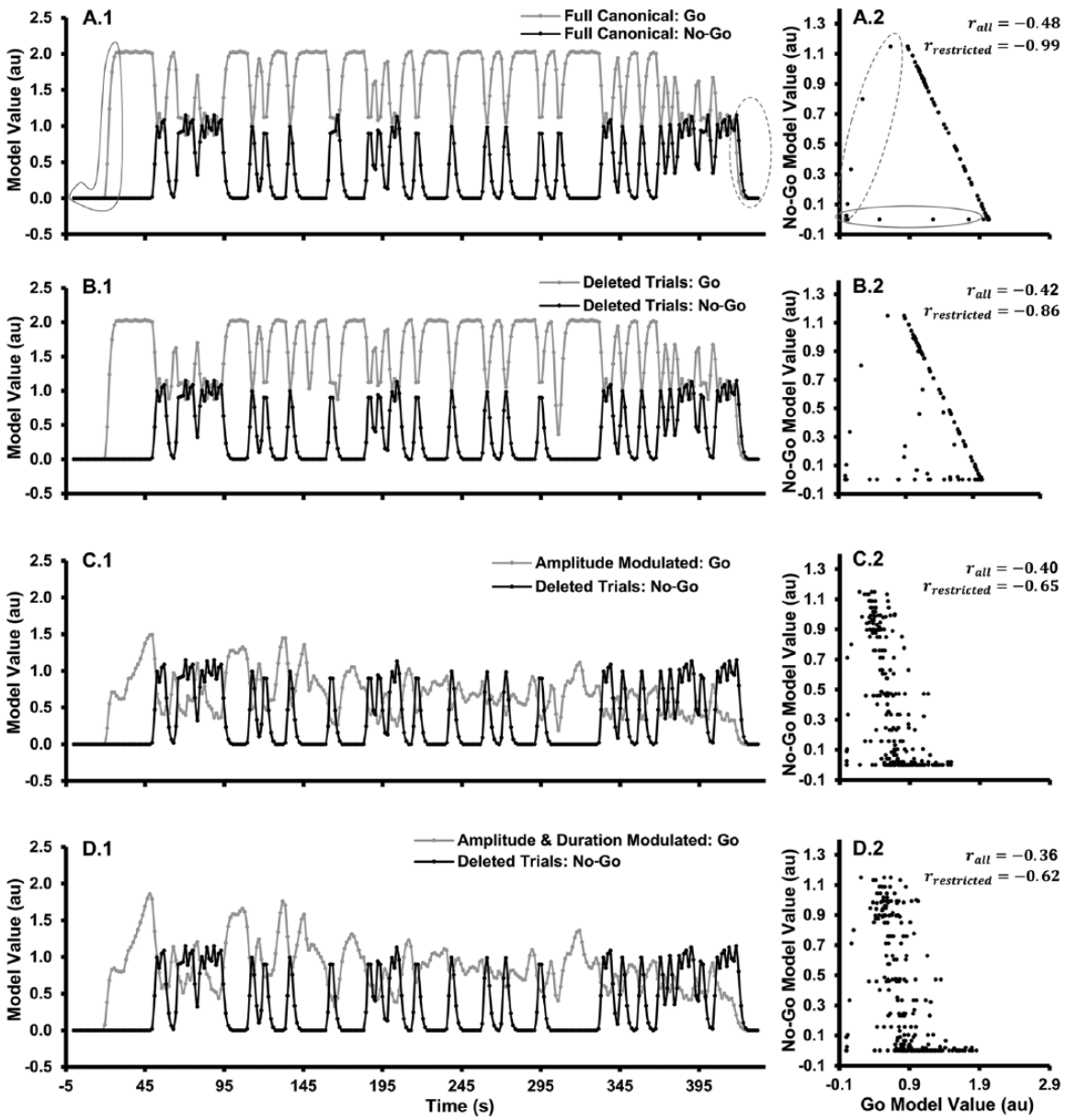

Figure 1. *Go* and *no-go* regressors and scatterplots showing correlations between regressors. Regressors were created by convolving a γ-variate function with δ-functions depicting *go* and *no-go* stimulus onsets: (A.1) with all trials included, (B.1) after deleting incorrect trials and trials with outlier reaction times (RT), (C.1) after modulating the amplitudes of the *go* δ-functions by RT, and (D.1) after modulating the amplitude and width of the δ-functions by RT. In the figures on the left, *go* regressors are depicted in gray, and *no-go* regressors are depicted in black. Scatterplots and correlation coefficients showing relationships between the regressors are shown to the right of the respective models (A.2-D.2). Points circled in solid and dashed gray lines (A.1 and A.2) are outliers having undue influence on the linear relationships between the *go* and *no-go* regressors, and correlation coefficients between the *go* and *no-go* regressors both with (ie, r_{all}) and without (ie, $r_{restricted}$) these data points are shown in the respective scatterplots.

were convolved with the HRF. For all of the regressors, data points corresponding to those deviating from the negative correlations between the full-model *go* and *no-go* regressors (see above and Figure 1A.1 and 1A.2) were deemed outliers, having undue influence on the accurate estimation of the linear relationships between the *go* and *no-go* regressors and were excluded from further analysis. In total, 17 points were dropped from the beginning and 11 from the end (circled points in Figure 1A.1 and 1A.2) of the regressors and time series.

Comparisons of the *go* regressors (gray) illustrate the changes in the models from the full canonical *go* regressor (Figure 1A.1) due to DT (Figure 1B.1), AM (Figure 1C.1), and A&DM (Figure 1D.1) of the *go* models. Comparisons of changes in the correlations between the *go* and *no-go* (black) models illustrate the increased independence of the *no-go* regressor from the *go* regressor due to dropping trials and RT modulation of the *go* regressor. Across models created for the participants, the shared variance (R^2) between the *go* and *no-go* regressors was significantly lower for the A&DM ($-.87 \leq r \leq -.35$; mean $R^2 = 0.53$) than for AM ($-.90 \leq r \leq -.41$; mean $R^2 = 0.57$) and for DT ($-.94 \leq r \leq -.72$; mean $R^2 = 0.74$) models, $F_{2,30} = 41.00$, $P < .05$, and all t's$(15) \geq 5.60$, P's$\leq .05$

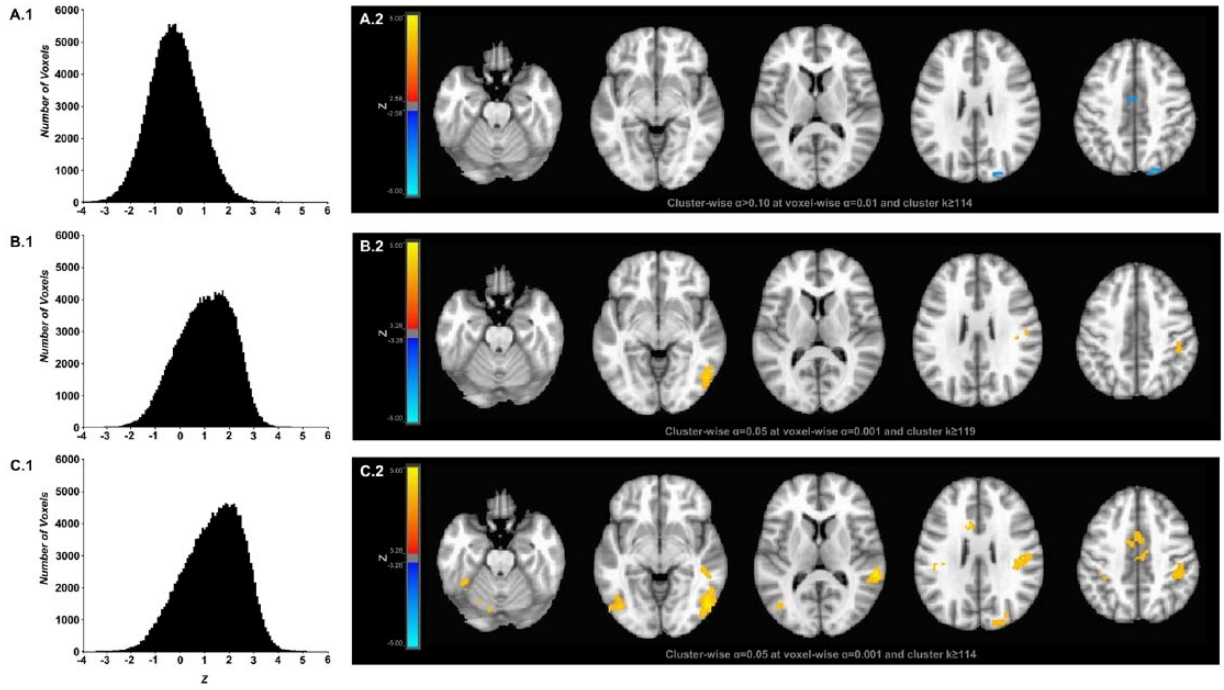

Figure 2. Histograms and statistical parameter maps showing distributions of *z* values and clusters of significant signal-change for *no-go* trials when deleted trial (A.1 and A.2), amplitude-modulated (B.1 and B.2), and amplitude and duration–modulated *go* regressors were included in the regression analyses. (A.1) Histogram of *z* values from all voxels used in the group-level analyses and corresponding (A.2) color-scaled, 1-sample, *z*-statistic maps for *no-go* percent signal-change estimates obtained via regression modeling with *go* and *no-go* regressors having incorrect and outlier reaction time (RT) trials deleted. As shown, lower voxel-wise and cluster-wise statistical criteria were used for the deleted trials modeling because no significant effects were found when family-wise error–corrected criteria were used (see text). (B.1) Histogram of *z* values from all voxels used in the group-level analyses and corresponding (B.2) color-scaled, 1-sample, *z*-statistic maps for *no-go* percent signal-change estimates obtained via regression modeling that included the RT-based amplitude-modulated *go* regressor. (C.1) Histogram of *z* values from all voxels used in the group-level analyses and corresponding (C.2) color-scaled, 1-sample, *z*-statistic maps for *no-go* percent signal-change estimates obtained via regression modeling that included the RT-based amplitude and duration–modulated *go* regressor. For all 1-sample *z* statistic, *no-go* mean percent signal-change was compared with 0. Positive values in the histograms and red-yellow voxels on *z*-statistic maps indicate that the mean percent signal-change was greater than 0, and negative values in the histograms and blue-cyan voxels on *z*-statistic maps indicate that the mean percent signal-change was less than 0. Brain images shown in neurological convention, right=right.

(Figure 1B.2 to 1D.2). Thus, amplitude and duration modulation of the *go* regressor reduced the collinearity between the *go* and *no-go* regressors to a greater degree than amplitude modulation alone and deleting trials, although amplitude modulation alone also reduced the collinearity between the *go* and *no-go* regressors to a greater degree than just deleting trials.

The degree of collinearity between the *go* and *no-go* regressors for each type of *go* regressor also was related to the behavioral measures used to induce variability between the regressors. The strength of the correlations between the *go* and *no-go* regressors for the DT regressor, but not for the AM and A&DM regressors, was significantly correlated with the number of DTs ($r(n=16)=.73$, $P<.05$; $r(n=16)=.001$; and $r(n=16)=.05$, respectively). However, the strength of the correlations between the *go* and *no-go* regressors for the AM and A&DM regressors, but not for the DT regressor, was significantly correlated with mean RT and with coefficient of variation ($r(n=16)=.53$, $P<.05$; $r(n=16)=.52$, $P<.05$ and $r(n=16)=.28$, respectively; SD_{RT}/M_{RT} $r(n=16)=.71$, $P<.05$; $r(n=16)=.70$, $P<.05$; and $r(n=16)=.13$, respectively). Thus, deleting trials, longer mean RT, and greater RT variability led to reductions in the collinearity between the *go* and *no-go* regressors, but with the AM and A&DM regressors, longer mean RT and greater RT variability were key to reducing the collinearity.

Evaluation of "Detected" No-Go Effects

Imaging analyses were performed using AFNI software.[20] The data for individual participants were corrected for slice-timing offset and motion, spatially smoothed (Gaussian kernel full width at the half maximum = 8 mm), and scaled so that the deconvolution parameter estimates would be expressed in terms of percent signal-change (ie, $100^*y(t)/M(y)$, where $y(t)$ is the BOLD signal in a given voxel at time t in the time series and $M(y)$ is the mean of the time series within that voxel). Three separate percent signal-change estimates for the *no-go* responses were then obtained through separate regression analyses for models that included the DT, AM, and A&DM *go* regressors. Nuisance regressors for the motion correction parameters and linear, quadratic, and cubic trends were included in the regression models. The 3 *no-go* percent signal-change matrices obtained for each participant were spatially normalized (resampled to a 2-mm isovoxel resolution) to Talairach space.[21] The high-resolution anatomical image was registered

Table 1. Descriptive statistics for clusters found for analyses including different *go* regression models.

MODEL	CLUSTER SIZE	PEAK VOXEL				
		Z VALUE	TALAIRACH COORDINATES			BRAIN REGION
			X	*Y*	*Z*	
Deleted trials[a]	141	−4.05	25	−81	36	Right occipital-parietal BA7/19
	138	−4.14	9	−3	36	Right cingulate BA24
Amplitude modulated	185	4.01	43	−23	34	Right inferior parietal BA40
	173	4.20	49	−63	−4	Right occipital-temporal BA19/37
Amplitude and duration modulated	1837	5.14	59	−31	14	Right superior temporal BA22
	491	4.65	−39	−43	−26	Left cerebellum
	310	4.89	−11	13	28	Left cingulate BA24
	253	4.24	−51	−71	−4	Left occipital-temporal BA19/37
	156	3.94	31	−83	22	Right occipital BA19
	137	3.90	−13	−51	52	Left parietal BA7
	131	4.16	−45	−27	28	Left inferior parietal BA40
	120	4.46	21	−67	52	Right parietal BA7

Abbreviation: BA, Brodmann area.
[a]For the deleted trials model, the voxel-wise $\alpha = .01$ (raised from voxel-wise $\alpha = .001$ for the amplitude-modulated and amplitude and duration–modulated models) and the 2 clusters were not significant at cluster-wise $\alpha = .05$.

with an anatomical template via 6-parameter affine transformation and subsequent nonlinear registration, using FLIRT and FNIRT in FSL v4.1.5,[22] and the transformation parameters were then applied to the percent signal-change matrices. Group-level analyses were performed on the spatially normalized percent signal-change matrices. Group-level analyses consisted of voxel-wise 1-sample *z* statistics calculated to determine which brain regions showed significant, group-level *no-go* effects for the different regression models. Cluster thresholding to control family-wise error (FWE) rates involved computing residuals for the contrast of interest, generating a null distribution by randomizing the signs of the residuals per subject, iteratively ($k = 10\,000$) generating *z* statistics on the residual matrices, and then using the *z*-statistic matrices to determine false-positive probabilities of clusters of a given size with different voxel-wise *P* value thresholds,[23] thus addressing concerns regarding inflated false-positive rates in fMRI studies.[24]

Voxel-wise 1-sample *z* statistics were calculated to determine which brain regions showed significant, group-level *no-go* effects when the DT, AM, and D&AM *go* models were included in the subject-level regression analyses. Histograms of the distributions of *z* values extracted from all voxels included in a whole brain mask ($k = 167\,149$ voxels) show that the distribution was negatively shifted from 0 for analyses that included the DT model (Figure 2A.1) but positively shifted from 0 for the analyses that included the AM (Figure 2B.1) and D&AM (Figure 2C.1) models. After FWE correction, the analyses with the DT model failed to show significant clusters associated with *no-go* trials. At a reduced threshold, however, voxel-wise $P < .01$ (reduced only for the analysis of *no-go* effects when the DT model was included), clusters of *no-go*–related negative signal-change were observed in right parietal ($k = 141$) and right cingulate ($k = 138$) regions (Figure 2A.2 and Table 1). After FWE correction, for the analysis with the AM model, 2 significant clusters were observed (Figure 2B.2 and Table 1), both showing positive signal-change. One cluster ($k = 185$) extended from right inferior parietal cortex (BA40) to right precentral gyrus, and the other

cluster ($k = 173$) was in the right occipital-temporal region (BA37). For the D&AM model, 8 significant clusters at the FWE-corrected threshold were observed (Figure 2C.2 and Table 1), and all showed positive signal-change. A large cluster ($k = 1836$ voxels), with a peak z value within right superior temporal gyrus, extended from inferior parietal cortex (BA40) ventrally across middle temporal gyrus to the occipito-temporal region (BA37). Both of the clusters found for the analysis including the AM model were encompassed within this large cluster. The 7 additional clusters only were observed when the D&AM model was included—first ($k = 491$) extended on the left from the cerebellum into inferior temporal cortex, second ($k = 310$) was within left cingulate cortex (BA24), third ($k = 253$) encompassed the left occipito-temporal junction (BA37), fourth ($k = 156$) was at the right occipito-parietal junction, fifth ($k = 137$) was within left superior temporal cortex (BA7), sixth ($k = 131$) was within left inferior parietal cortex (BA40), and seventh ($k = 120$) was within right superior temporal cortex (BA7).

Conclusions

The results show the efficacy of using RT-based modulation in the regression analysis of fMRI data to reduce collinearity between regressors when invariant SDTs and ITIs are required to elicit the engagement of targeted cognitive processes. In addition to reducing collinearity between the *go* and *no-go* regressors, RT modulation improved the detection of *no-go* effects in group-level analyses. In fact, without RT modulation, significant *no-go* effects were not detected when conventional FWE-correction criteria were applied. In addition, RT-based amplitude and duration modulation of the *go* regressor led to the detection of more clusters showing significant *no-go*–related signal-change.

The results suggest that other trial-level measures (eg, RTs from binary responses) can be used to build modulated regressors and increase regressor independence when invariant SDTs and ITIs are required, assuming that the measures are more accurate indices of the timing of the cognitive processes of interest than, for instance, SDTs. However, when RT-based modulation was used, the association between the *go* and *no-go* regressors was found to vary with mean RT and RT variability. The correlations then suggest potential limitations in the use of the modulation approach. For example, group differences in potential regressor modulator means or variabilities could differentially bias the ability to detect signal-change in the groups, and such biases could then lead to artifactual group differences or contribute to error in estimating differences in signal-change magnitudes between groups. Thus, the potential of moderators to induce artifactual group or condition differences in BOLD signal-change estimates needs to be carefully considered.

Author Contributions

MAM wrote the manuscript.
All authors contributed to editing the manuscript.
MAK, JH, and HSC developed the initial study.
HSC collected the data.
MAM, NKR, ES-K, and HSC developed the analysis plan and analyzed the data.

REFERENCES

1. Altmann EM. The preparation effect in task switching: carryover of SOA. *Mem Cognit*. 2004;32:153–163.
2. Bherer L, Belleville S. Age-related differences in response preparation: the role of time uncertainty. *J Gerontol B Psychol Sci Soc Sci*. 2004;59:66–74.
3. Polzella DJ, Ramsey EG, Bower SM. The effects of brief variable foreperiods on simple reaction time. *Bullet Psyc Soc*. 1989;27:467–469.
4. Ryan M, Martin R, Denckla MB, Mostofsky SH, Mahone EM. Interstimulus jitter facilitates response control in children with ADHD. *J Int Neuropsychol Soc*. 2010;16:388–393.
5. Vaurio RG, Simmonds DJ, Mostofsky SH. Increased intra-individual reaction time variability in attention-deficit/hyperactivity disorder across response inhibition tasks with different cognitive demands. *Neuropsychologia*. 2009;47:2389–2396.
6. Wodka EL, Simmonds DJ, Mahone EM, Mostofsky SH. Moderate variability in stimulus presentation improves motor response control. *J Clin Exp Neuropsychol*. 2009;31:483–488.
7. Cohen MS. Parametric analysis of fMRI data using linear systems methods. *Neuroimage*. 1997;6:93–103.
8. Heuttel SA, Song AW, McCarthy G. *Functional Magnetic Resonance Imaging*. 2nd ed. Sunderland, MA: Sinauer Associates, Inc.; 2004.
9. Mason CH, Perreault WD. Collinearity power and interpretation of multiple-regression analysis. *J Market Res*. 1991;28:268–280.
10. Mela CF, Kopalle PK. The impact of collinearity on regression analysis: the asymmetric effect of negative and positive correlations. *Appl Econom*. 2002;34:667–677.
11. Buchsbaum BR, Greer S, Chang WL, Berman KF. Meta-analysis of neuroimaging studies of the Wisconsin card-sorting task and component processes. *Hum Brain Mapp*. 2005;25:35–45.
12. Simmonds DJ, Pekar JJ, Mostofsky SH. Meta-analysis of Go/No-go tasks demonstrating that fMRI activation associated with response inhibition is task-dependent. *Neuropsychologia*. 2008;46:224–232.
13. Durston S, Thomas KM, Worden MS, Yang Y, Casey BJ. The effect of preceding context on inhibition: an event-related fMRI study. *Neuroimage*. 2002;16:449–453.
14. Braver TS, Barch DM, Gray JR, Molfese DL, Snyder A. Anterior cingulate cortex and response conflict: effects of frequency, inhibition and errors. *Cereb Cortex*. 2001;11:825–836.
15. Williams LM, Simms E, Clark CR, Paul RH, Rowe D, Gordon E. The test-retest reliability of a standardized neurocognitive and neurophysiological test battery: "neuromarker." *Int J Neurosci*. 2005;115:1605–1630.
16. Helsdingen AS, van Gog T, van Merriënboer JJG. The effects of practice schedule on learning a complex judgment task. *Learn Instr*. 2011;21:126–136.
17. Grinband J, Wager TD, Lindquist M, Ferrera VP, Hirsch J. Detection of time-varying signals in event-related fMRI designs. *Neuroimage*. 2008;43:509–520.
18. Chiang HS, Motes MA, Mudar RA, et al. Semantic processing and response inhibition. *Neuroreport*. 2013;24:889–893.
19. Snodgrass JG, Vanderwart M. A standardized set of 260 pictures: norms for name agreement, image agreement, familiarity, and visual complexity. *J Exp Psychol Hum Learn*. 1980;6:174–215.
20. Cox RW. AFNI: software for analysis of visualization of functional magnetic resonance neuroimages. *Comput Biomed Res*. 1996;29:162–173.
21. Talairach J, Tournoux P. *Co-planar Stereotaxic Atlas of the Human Brain*. New York, NY: Thieme Medical Publishers; 1988.
22. Smith SM, Jenkinson M, Woolrich MW, et al. Advances in functional and structural MR image analysis and implementation as FSL. *Neuroimage*. 2004;23:S208–S219.
23. Cox RW, Chen G, Glen DR, Reynolds RC, Taylor PA. FMRI clustering in AFNI. False-positive rates redux. *Brain Connectivity*. 2017;7:152–171.
24. Eklund A, Nichols TE, Knutsson H. Cluster failure: why fMRI inferences for spatial extent have inflated false-positive rates. *Proc Natl Acad Sci U S A*. 2017;113:7900–7905.